

Baryon asymmetry via leptogenesis in a neutrino mass model with complex scaling

Rome Samanta^{a*}, Mainak Chakraborty^{b†}, Probir Roy^{c‡}, Ambar Ghosal^{a§}

- a) Saha Institute of Nuclear Physics, HBNI, 1/AF Bidhannagar, Kolkata 700064, India
- b) Centre of Excellence in Theoretical and Mathematical Sciences, SOA University, Khandagiri Square, Bhubaneswar 751030, India
- c) Center for Astroparticle Physics and Space Science, Bose Institute, Kolkata 700091, India

March 7, 2017

Abstract

Baryogenesis via leptogenesis is investigated in a specific model of light neutrino masses and mixing angles. The latter was proposed on the basis of an assumed complex-extended scaling property of the neutrino Majorana mass matrix M_ν , derived with a type-1 seesaw from a Dirac mass matrix m_D and a heavy singlet neutrino Majorana mass matrix M_R . One of its important features, highlighted here, is that *there is a common source of the origin of a nonzero θ_{13} and the CP violating lepton asymmetry through the imaginary part of m_D* . The model predicted CP violation to be maximal for the Dirac type and vanishing for the Majorana type. We assume strongly hierarchical mass eigenvalues for M_R . The leptonic CP asymmetry parameter ε_1^α with lepton flavor α , originating from the decays of the lightest of the heavy neutrinos N_1 (of mass M_1) at a temperature $T \sim M_1$, is what matters here with the lepton asymmetries, originating from the decays of $N_{2,3}$, being washed out. The light leptonic and heavy neutrino number densities (normalized to the entropy density) are evolved via Boltzmann equations down to electroweak temperatures to yield a baryon asymmetry through sphaleronic transitions. The effects of flavored vs. unflavored leptogenesis in the three mass regimes (1) $M_1 < 10^9$ GeV, (2) 10^9 GeV $< M_1 < 10^{12}$ GeV and (3) $M_1 > 10^{12}$ GeV are numerically worked out for both a normal and an inverted mass ordering of the light neutrinos. Corresponding results on the baryon asymmetry of the universe are obtained, displayed and discussed. For values close to the best-fit points of the input neutrino mass and mixing parameters, obtained from neutrino oscillation experiments, successful baryogenesis is achieved for the mass regime (2) and a normal mass ordering of the light neutrinos with a nonzero θ_{13} playing a crucial role. However, the other possibility of an inverted mass ordering for the same mass regime, though disfavored, cannot be excluded. A discussion is also given on the sensitivity of our result to the masses $M_{2,3}$ of the heavier neutrinos $N_{2,3}$.

*rome.samanta@saha.ac.in

†mainak.chakraborty2@gmail.com

‡probirrana@gmail.com

§ambar.ghosal@saha.ac.in

1 Introduction

Much effort has already been made towards understanding the origin of the baryon asymmetry of the universe $Y_B = (n_B - n_{\bar{B}})/s \simeq (8.7 \pm 0.1) \times 10^{-11}$ [1] – the number density (n_B) of baryons minus that ($n_{\bar{B}}$) of antibaryons normalized to the entropy density s . A comprehensive review with references may be found in Ref. [2]. Various possible mechanisms have been considered for this purpose, e.g. GUT baryogenesis, electroweak baryogenesis, the Affleck-Dine mechanism and baryogenesis via leptogenesis. We concentrate on the last-mentioned possibility [3–8]. Here a CP odd particle-antiparticle asymmetry is first generated at a high scale in the leptonic sector; that is thereafter converted into a baryon asymmetry by sphaleron processes during the electroweak phase transition. In the most popular extension of the Standard Model (SM) for generating light neutrino masses, three¹ heavy right-chiral (RH) singlet neutrinos are added to induce tiny neutrino masses and their mixing angles through the type-1 seesaw mechanism [9–12]. The complex Yukawa couplings $f_{i\alpha}^N$, that connect those singlet RH neutrinos N_i to the SM-doublet left-chiral leptons of flavor α , generate the necessary CP violation in the decays of those heavy RH neutrinos into the Higgs scalar plus the SM leptons. The occurrence of Majorana mass terms for the heavy neutrinos in the Lagrangian provides the required lepton nonconservation. The rate of interaction with those Yukawa couplings being smaller than the Hubble expansion rate, departure from thermal equilibrium ensues. Hence all the Sakharov conditions [13] are fulfilled for generating Y_B . The present work is devoted to a quantitative study of the origin of Y_B via leptogenesis in a model [14,15] of neutrino masses with complex scaling – proposed by some of us. As a step towards that, we shall summarize the relevant features of the concerned model in the next Sec. 2.

First, let us establish our notation and convention by choosing without loss of generality the Weak Basis (sometimes called the leptogenesis basis [16]) in which the 3×3 mass matrices, not only of the charged leptons but also of the heavy RH neutrinos, are diagonal with nondegenerate real and positive entries, e.g. $M_R = \text{diag}(M_1, M_2, M_3)$, M_i ($i = 1, 2, 3$) > 0 . We shall work in the strongly hierarchical scenario in the right-chiral neutrino sector in which those masses will be taken to be widely spaced. Specifically, we assume that $M_1 \ll M_2 \ll M_3$. A crucial input into these scenarios is the flavor structure of the neutrino Dirac mass matrix m_D . The latter appears in the neutrino mass terms of the Lagrangian as

$$-\mathcal{L}_{mass}^{\nu,N} = \bar{N}_{iR}(m_D)_{i\alpha}\nu_{L\alpha} + \frac{1}{2}\bar{N}_{iR}(M_R)_i\delta_{ij}N_{jR}^C + \text{h.c.} \quad (1.1)$$

with $N_j^C = CN_j^T$. The effective light neutrino Majorana mass matrix M_ν is then given by the standard seesaw result [9–12]

$$M_\nu = -m_D^T M_R^{-1} m_D. \quad (1.2)$$

This M_ν enters the effective low energy neutrino mass term in the Lagrangian as

$$-\mathcal{L}_{mass}^\nu = \frac{1}{2}\nu_{L\alpha}^{\bar{C}}(M_\nu)_{\alpha\beta}\nu_{L\beta} + \text{h.c.} \quad (1.3)$$

It is a complex symmetric 3×3 matrix ($M_\nu^* \neq M_\nu = M_\nu^T$) which can be put into a diagonal form by a similarity transformation with a unitary matrix U :

$$U^T M_\nu U = M_\nu^d \equiv \text{diag}(m_1, m_2, m_3) \quad (1.4)$$

with m_i ($i = 1, 2, 3$) taken to be nonzero, real and small positive masses $< \mathcal{O}(\text{eV})$. In our Weak Basis we can take U as

$$U = U_{PMNS} \equiv \begin{pmatrix} c_{12}c_{13} & e^{i\frac{\alpha}{2}}s_{12}c_{13} & s_{13}e^{-i(\delta-\frac{\beta}{2})} \\ -s_{12}c_{23} - c_{12}s_{23}s_{13}e^{i\delta} & e^{i\frac{\alpha}{2}}(c_{12}c_{23} - s_{12}s_{13}s_{23}e^{i\delta}) & c_{13}s_{23}e^{i\frac{\beta}{2}} \\ s_{12}s_{23} - c_{12}s_{13}c_{23}e^{i\delta} & e^{i\frac{\alpha}{2}}(-c_{12}s_{23} - s_{12}s_{13}c_{23}e^{i\delta}) & c_{13}c_{23}e^{i\frac{\beta}{2}} \end{pmatrix} \quad (1.5)$$

with $c_{ij} \equiv \cos\theta_{ij}$, $s_{ij} \equiv \sin\theta_{ij}$ and $\theta_{ij} = [0, \pi/2]$. CP violation enters here through nonzero values of the Dirac phase δ and of the Majorana phases α, β with $\delta, \alpha, \beta = [0, 2\pi]$. We follow the PDG convention [17] on these angles and phases except that we denote the Majorana phases by α and β .

In the main body of the paper we calculate the CP asymmetry originating from the decays $N_i \rightarrow \bar{L}_\alpha\phi$, $L_\alpha^C\phi^\dagger$ where L_α and ϕ are the respective fields of the SM left-chiral lepton doublet of flavor α and the Higgs doublet. This is done in terms of the imaginary parts of appropriately defined quartic products of the neutrino Dirac mass matrix m_D and its hermitian conjugate m_D^\dagger , as well as of an explicit function of the variable $x_{ij} \equiv M_j^2/M_i^2$. Clearly, the calculation depends sensitively on the flavor structure of m_D and hence on the specific neutrino mass model under consideration. The CP asymmetries (and therefore

¹This can be done with two heavy RH singlet neutrinos but not with just one.

leptogenesis as a whole) may be flavor dependent or independent according to the temperature regime in which the CP violating decays take place. For an evolution down to the electroweak scale, one needs to solve the corresponding Boltzmann Equations. We therefore consider the Boltzmann evolution equation for the number density n_a of a particle of type a (either a right-chiral heavy neutrino N_i or a left-chiral lepton doublet \mathcal{L}_α) normalized to the photon number density n_γ . For this purpose, we take

$$\eta_a(z) = \frac{n_a(z)}{n_\gamma(z)}, n_\gamma(z) = \frac{2M_1^3}{\pi^2 z^3} \quad (1.6)$$

as functions of $z \equiv M_1/T$. We rewrite these equations for the variable Y_a where

$$Y_a = n_a/s = \frac{n_\gamma}{s}\eta_a = 1.8g_{*s}\eta_a, \quad (1.7)$$

g_{*s} being the total number of effective and independent massless degrees of freedom at the concerned temperature. The evolution of Y_a is studied for different a 's from a temperature of the order of the lightest right-chiral neutrino mass M_1 to that of the electroweak phase transition where sphaleron-induced processes take place converting the lepton asymmetry into a baryon asymmetry Y_B .

In pursuing Y_B , we need to zero in on Y_{Δ_λ} where $\Delta_\lambda = \frac{1}{3}B - L_\lambda$ with B being the baryon number and L_λ the lepton number of the active flavor λ . The analysis is done numerically but in three different regimes [7,8] depending on where M_1 lies: (1) $M_1 < 10^9$ GeV where all the lepton flavor are distinctly active, (2) 10^9 GeV $< M_1 < 10^{12}$ GeV where e and μ flavors are indistinguishable but the τ -flavor is separately active and (3) $M_1 > 10^{12}$ GeV where all lepton flavors are indistinguishable. The quantity Y_B and Y_{Δ_λ} are linearly related but with different numerical coefficients for the three different regimes. In our numerical analysis, six constraints from experimental and observational data are inputted: the 3σ ranges of the solar and atmospheric neutrino mass squared differences as well as of the three neutrino mixing angles plus the cosmological upper bound on the sum of the three light neutrino masses. The analysis is done separately in each regime for a normal mass ordering ($m_3 > m_2 > m_1$) as well as for an inverted ordering ($m_2 > m_1 > m_3$) of the light neutrinos. The final results are tabulated numerically as well as displayed graphically.

We have already mentioned the content of Section 2. The rest of the paper is organized as follows. In Section 3 we calculate the CP asymmetry parameters generated in the decays of N_i into $\mathcal{L}_\alpha\phi$ and $\mathcal{L}_\alpha^C\phi^\dagger$. Section 4 contains an algebraic treatment of the Boltzmann evolution equations and of the generation of the baryon asymmetry Y_B in the three mass regimes. The numerical analysis that follows is detailed with a discussion of its consequences in Section 5. Section 6 addresses the possible role played by the heavier neutrinos $N_{2,3}$. A summary of our work is given in the last Section 7.

2 Complex scaling with type-I seesaw

A key feature of M_ν is the $\mathbb{Z}_2 \times \mathbb{Z}_2$ residual symmetry [18] that it possesses. This is an invariance of M_ν under a linear transformation on neutrino fields

$$\nu_{L\alpha} \rightarrow G_{\alpha\beta}\nu_{L\beta}, \quad (2.1)$$

i.e. in a matrix notation, with a 3×3 matrix G ,

$$G^T M_\nu G = M_\nu. \quad (2.2)$$

One can show [18] that there are two independent matrices $G^{2,3}$ implementing this invariance and obeying the unitary diagonalization

$$G^{2,3}U = Ud^{2,3}, \quad (2.3)$$

where $d^2 = \text{diag.} (-1, 1, 1)$ and $d^3 = \text{diag.} (-1, -1, 1)$. Some of us have proposed [14] a complex extension of this symmetry by considering the nonstandard CP transformations

$$\nu_{L\alpha} \rightarrow i(G_L)_{\alpha\beta}\gamma^0\nu_{L\beta}^C, \quad N_{Ri} \rightarrow i(G_R)_{ij}\gamma^0N_{Rj}^C \quad (2.4)$$

and demanding the invariance relations

$$G_R^\dagger m_D G_L = m_D^*, \quad G_R^\dagger M_R G_R^* = M_R^*. \quad (2.5)$$

Eqs. (1.2) and (2.5) together imply

$$G_L^T M_\nu G_L = M_\nu^* \quad (2.6)$$

which is our complex-extended invariance statement on the low energy neutrino Majorana mass matrix M_ν . At this point, G_L is taken to be [14]

$$G_L = G_3^{\text{scaling}} = \begin{pmatrix} -1 & 0 & 0 \\ 0 & (1-k^2)(1+k^2)^{-1} & 2k(1+k^2)^{-1} \\ 0 & 2k(1+k^2)^{-1} & -(1-k^2)(1+k^2)^{-1} \end{pmatrix} = (G_3^{\text{scaling}})^T, \quad (2.7)$$

k being a real scaling factor. This G_3^{scaling} is the operative residual symmetry generator for the original scaling ansatz [19–22]. It now obeys the relation

$$G_3^{\text{scaling}} U^* = U \tilde{d}, \quad (2.8)$$

where $\tilde{d}_{\alpha\beta}$ equals $\pm\delta_{\alpha\beta}$ and hence admits eight possibilities. Only four of these were shown [14] to be viable and led independently to the results

$$\tan\theta_{23} = k^{-1}, \quad (2.9)$$

$$\sin\alpha = \sin\beta = \cos\delta = 0. \quad (2.10)$$

The detailed phenomenological consequences of (2.9) and (2.10) were worked out in Ref. [14]. The most general M_ν , that satisfies

$$(G_3^{\text{scaling}})^T M_\nu G_3^{\text{scaling}} = M_\nu^*, \quad (2.11)$$

is given by the complex-extended scaling (CES) form of M_ν , namely [14]

$$M_\nu^{CES} = \begin{pmatrix} x & -y_1 k + i y_2 k^{-1} & y_1 + i y_2 \\ -y_1 k + i y_2 k^{-1} & z_1 - w k^{-1}(k^2 - 1) - i z_2 & w - i z_2 (2k)^{-1}(k^2 - 1) \\ y_1 + i y_2 & w - i z_2 (2k)^{-1}(k^2 - 1) & z_1 + i z_2 \end{pmatrix}, \quad (2.12)$$

where x , $y_{1,2}$, $z_{1,2}$ and w are real mass dimensional quantities.

Since M_R has been taken to be diagonal, the corresponding symmetry generator matrix G_R , cf. the second of Eqs. (2.5), is diagonal with entries ± 1 , i.e.

$$G_R = \text{diag}(\pm 1, \pm 1, \pm 1). \quad (2.13)$$

Thus there are eight different structures of G_R . Correspondingly, from the first relation of (2.5), there could be eight possible different structures of m_D . It can be shown by tedious algebra that all other structures of G_R , except for

$$G_R = \text{diag}(-1, -1, -1), \quad (2.14)$$

are incompatible with scaling symmetry [19]. Thus we take G_R of (2.14) as the only viable residual symmetry of M_R . We can now write the first of (2.5) as

$$m_D G_L = -m_D^* \quad (2.15)$$

which is really a complex extension of the Joshipura-Rodejohann result² [23] $m_D G_L = -m_D$.

The most general form of m_D that satisfies (2.15) is

$$m_D^{CES} = \begin{pmatrix} a & b_1 + i b_2 & -b_1/k + i b_2 k \\ e & c_1 + i c_2 & -c_1/k + i c_2 k \\ f & d_1 + i d_2 & -d_1/k + i d_2 k \end{pmatrix}, \quad (2.16)$$

where a , $b_{1,2}$, $c_{1,2}$, $d_{1,2}$, e and f are nine a priori unknown real mass dimensional quantities apart from the real, positive, dimensionless k . Using (1.2), M_ν^{CES} of (2.12) obtains with the real mass parameters x , $y_{1,2}$, $z_{1,2}$ and w related to those of (2.16), as given in Table 1. It is noteworthy that whereas m_D^{CES} has ten real parameters, M_ν^{CES} has only seven.

Table 1: Parameters of M_ν^{CES} in terms of the parameters of m_D and M_R .

$x = -\left(\frac{a^2}{M_1} + \frac{e^2}{M_2} + \frac{f^2}{M_3}\right)$ $y_1 = \frac{1}{k} \left(\frac{ab_1}{M_1} + \frac{ec_1}{M_2} + \frac{fd_1}{M_3}\right)$ $y_2 = k \left(\frac{ab_2}{M_1} + \frac{ec_2}{M_2} + \frac{fd_2}{M_3}\right)$ $z_1 = -\frac{1}{k^2} \left(\frac{b_1^2}{M_1} + \frac{c_1^2}{M_2} + \frac{d_1^2}{M_3}\right) + k^2 \left(\frac{b_2^2}{M_1} + \frac{c_2^2}{M_2} + \frac{d_2^2}{M_3}\right)$ $z_2 = \frac{2b_1 b_2}{M_1} + \frac{2c_1 c_2}{M_2} + \frac{2d_1 d_2}{M_3}$ $w = \frac{1}{k} \left(\frac{b_1^2}{M_1} + \frac{c_1^2}{M_2} + \frac{d_1^2}{M_3}\right) + k \left(\frac{b_2^2}{M_1} + \frac{c_2^2}{M_2} + \frac{d_2^2}{M_3}\right)$

²Those authors followed a different phase convention; they obtained $m_D G_L = m_D$ instead of $m_D G_L = -m_D$.

One can count the real parameters, as given in m_D of (2.16). Along with the RH neutrino masses M_1, M_2, M_3 , one obtains a set of thirteen real parameters for M_ν . In order to reduce the number of parameters towards attaining the goal of a tractable result, we first use the assumed hierarchical nature of the RH neutrino masses $M_1 \ll M_2 \ll M_3$. We then take the parameters $d_{1,2}, e$ and f in Table 1 to be of the same order of magnitude as $a, b_{1,2}$ and $c_{1,2}$. That enables us to neglect all terms in Table 1 with M_3 in the denominator. Now we rescale the remaining parameters of Table 1 as follows:

$$a \longrightarrow a' = \frac{a}{\sqrt{M_1}}, \quad (2.17)$$

$$b_{1,2} \longrightarrow b'_{1,2} = \frac{b_{1,2}}{\sqrt{M_1}}, \quad (2.18)$$

$$c_{1,2} \longrightarrow c'_{1,2} = \frac{c_{1,2}}{\sqrt{M_2}}, \quad (2.19)$$

$$e \longrightarrow e' = \frac{e}{\sqrt{M_2}}. \quad (2.20)$$

Consequently, the entries of Table 1 can be written in terms of the rescaled parameters as in Table 2. We are now left with a six-dimensional parameter space with the real parameters $x, y_{1,2}, z_{1,2}$ and w as given in Table 2. Note that, had we neglected the terms with M_2 in the denominator too, we would have been left with a three dimensional parameter space which would have been in a danger of being overdetermined by the six experimental and observational constraints mentioned in the Introduction. We shall later discuss how to estimate the missing parameters f and $d_{1,2}$.

Table 2: Parameters of m_D^{CES} in the rescaled version.

$$\begin{aligned} x &= -(a'^2 + e'^2) \\ y_1 &= \frac{1}{k}(a'b'_1 + e'c'_1) \\ y_2 &= -k(a'b'_2 + e'c'_2) \\ z_1 &= -\frac{1}{k^2}(b_1'^2 + c_1'^2) + k^2(b_2'^2 + c_2'^2) \\ z_2 &= 2b_1'b'_2 + 2c_1'c'_2 \\ w &= \frac{1}{k}(b_1'^2 + c_1'^2) + k(b_2'^2 + c_2'^2) \end{aligned}$$

Before concluding this section, let us make an important point. In the absence of any imaginary part of the matrix m_D^{CES} of (2.16), the seesaw relation (1.2) gives rise to the Generalized Real Scaling form of M_ν , namely [14]

$$M_\nu^{GRS} = \begin{pmatrix} x & -y_1 k & y_1 \\ -y_1 k & z_1 - w k^{-1}(k^2 - 1) & w \\ y_1 & w & z_1 \end{pmatrix} \quad (2.21)$$

with real mass-dimensional entries. However, as was explained in Ref. [14], in this case θ_{13} vanishes and so information about the Dirac CP violating phase δ is lost. Moreover, owing to the real nature of the associated m_D^{GRS} , there is no Majorana CP violation either. Thus we see that the imaginary part of m_D^{CES} is the common source of an operative nonzero θ_{13} as well as CP violation in leptonic sector. The latter is in fact crucial to leptogenesis which is effected through a nonzero value of the CP asymmetry parameter ϵ , as explained in the next section. It is through the nonvanishing nature of $\text{Im } m_D^{CES}$ that the final matter-antimatter asymmetry in the universe gets directly related to the low energy parameters θ_{13} and δ .

3 Calculation of CP asymmetry parameter

The part of our Lagrangian relevant to the generation of a CP asymmetry is

$$-\mathcal{L}_D = f_{i\alpha}^N \bar{N}_{Ri} \tilde{\phi}^\dagger \mathcal{L}_\alpha + h.c., \quad (3.1)$$

where $\mathcal{L}_\alpha = (\nu_{L\alpha}, \ell_{L\alpha}^-)^T$ is the left-chiral SM lepton doublet of flavor α , while $\tilde{\phi} = (\phi^{0*}, -\phi^-)^T$ is the charge conjugated Higgs scalar doublet. It is evident from (3.1) that the decay products of N_i can be $\ell_\alpha^- \phi^+, \nu_\alpha \phi^0, \ell_\alpha^+ \phi^-$ and $\nu_\alpha^C \phi^{0*}$. We are interested in the flavor dependent CP asymmetry parameter ϵ_i^α which is given by

$$\epsilon_i^\alpha = \frac{\Gamma(N_i \rightarrow \mathcal{L}_\alpha \phi) - \Gamma(N_i \rightarrow \mathcal{L}_\alpha^C \phi^\dagger)}{\Gamma(N_i \rightarrow \mathcal{L}_\alpha \phi) + \Gamma(N_i \rightarrow \mathcal{L}_\alpha^C \phi^\dagger)}, \quad (3.2)$$

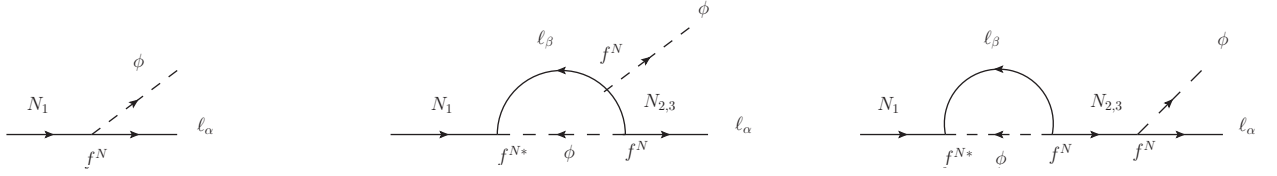


Figure 1: Tree level as well as one loop vertex correction and self energy diagrams that contribute to the CP asymmetry parameter ε_1^α . The flavor of the internal charged lepton ℓ_β is summed and the Yukawa coupling f^N is supplied with appropriate flavor indices in the interference amplitude.

Γ being the corresponding partial decay width. A nonzero value of ε_i^α needs to arise out of the interference between the tree level and one loop contributions [4]. This is since at the tree level we have

$$\Gamma^{tree}(N_i \rightarrow \ell_\alpha \phi) = \Gamma^{tree}(N_i \rightarrow \ell_\alpha^C \phi^\dagger) = (16\pi)^{-1} (f_{i\alpha}^{N\dagger} f_{i\alpha}^N) M_i, \quad (\text{no sum over } i). \quad (3.3)$$

One loop contributions come both from vertex correction and self-energy terms (cf. Fig.1). For leptogenesis with hierarchical heavy RH neutrinos, (3.2) can be evaluated to be

$$\varepsilon_i^\alpha = \frac{1}{4\pi v^2 \mathcal{H}_{ii}} \sum_{j \neq i} g(x_{ij}) \text{Im } \mathcal{H}_{ij}(m_D)_{i\alpha} (m_D^*)_{j\alpha} + \frac{1}{4\pi v^2 \mathcal{H}_{ii}} \sum_{j \neq i} \frac{\text{Im } \mathcal{H}_{ji}(m_D)_{i\alpha} (m_D^*)_{j\alpha}}{(1 - x_{ij})}. \quad (3.4)$$

In (3.4) $\langle \phi^0 \rangle = v/\sqrt{2}$ so that $m_D = v f^N / \sqrt{2}$, $\mathcal{H} \equiv m_D m_D^\dagger$ and x_{ij} was defined in Sec.1. Furthermore, $g(x_{ij})$ is given by

$$g(x_{ij}) = \frac{\sqrt{x_{ij}}}{1 - x_{ij}} + f(x_{ij}), \quad (3.5)$$

where the first RHS term arises from the one loop self energy term interfering with the tree level contribution. The second RHS term in (3.5), originating from the interference of the contribution from the one loop vertex correction diagram with the tree level term, is given by

$$f(x_{ij}) = \sqrt{x_{ij}} \left[1 - (1 + x_{ij}) \ln \left(\frac{1 + x_{ij}}{x_{ij}} \right) \right]. \quad (3.6)$$

Let us discuss some physics aspects of (3.4). As already mentioned, depending upon the temperature regime in which leptogenesis occurs, lepton flavors may be fully distinguishable, partly distinguishable or indistinguishable. It is reasonable to assume that leptogenesis takes place at $T \sim M_1$. It is known [4] that lepton flavors cannot be treated separately if the concerned process occurs above a temperature $T \sim M_1 > 10^{12}$ GeV. In case the said temperature is lower, two possibilities arise. When $T \sim M_1 < 10^9$ GeV all three (e, μ, τ) flavors are individually active and we need three CP asymmetry parameters $\varepsilon_i^e, \varepsilon_i^\mu, \varepsilon_i^\tau$ for each generation of RH neutrinos. On the other hand when we have $10^9 \text{ GeV} < T \sim M_1 < 10^{12}$ GeV, only the τ -flavor can be identified separately while the e and μ act indistinguishably. Here we need two CP asymmetry parameters $\varepsilon_i^{(2)} = \varepsilon_i^e + \varepsilon_i^\mu$ and ε_i^τ for each of the RH neutrinos. As an aside, let us point out a simplification in this model for unflavored leptogenesis which is relevant for the high temperature regime. Summing over all α ,

$$\sum_\alpha \text{Im } \mathcal{H}_{ji}(m_D)_{i\alpha} (m_D^*)_{j\alpha} = \text{Im } H_{ji} \mathcal{H}_{ij} = \text{Im } H_{ji} \mathcal{H}_{ji}^* = \text{Im } |\mathcal{H}_{ji}|^2 = 0, \quad (3.7)$$

i.e. the second term in the RHS of (3.4) vanishes. The flavor-summed CP asymmetry parameter is therefore given by the simplified expression

$$\begin{aligned} \varepsilon_i &= \sum_\alpha \varepsilon_i^\alpha \\ &= \frac{1}{4\pi v^2 \mathcal{H}_{ii}} \sum_{j \neq i} \left[f(x_{ij}) + \frac{\sqrt{x_{ij}}}{(1 - x_{ij})} \right] \text{Im } \mathcal{H}_{ij} \mathcal{H}_{ij}. \end{aligned} \quad (3.8)$$

In the mass model [14] being considered, it follows from (2.16) that

$$\mathcal{H}^{CES} = \begin{pmatrix} a^2 + b_1^2 p + b_2^2 q & ac + b_1 c_1 p + b_2 c_2 q & af + b_1 d_1 p + b_2 d_2 q \\ ac + b_1 c_1 p + b_2 c_2 q & e^2 + c_1^2 p + c_2^2 q & ef + c_1 d_1 p + c_2 d_2 q \\ af + b_1 d_1 p + b_2 d_2 q & ef + c_1 d_1 p + c_2 d_2 q & f^2 + d_1^2 p + d_2^2 q \end{pmatrix} \quad (3.9)$$

with $p = 1 + k^{-2}$ and $q = 1 + k^2$. Since (3.9) implies that $\text{Im } \mathcal{H}^{CES} = 0$, it follows from (3.8) that

$$\varepsilon_i = 0, \quad (3.10)$$

i.e. flavored-summed leptogenesis does not take place for any N_i . With the assumption that only the decay of N_1 matters in generating the CP asymmetry, ε_1 is the pertinent quantity for unflavored leptogenesis, but it vanishes. This nonoccurrence of unflavored leptogenesis is one of the robust predictions of the model.

Next, we focus on the calculation of the α -flavored CP asymmetry in terms of x_{12} , x_{13} and the elements of m_D^{CES} . These are relevant for the fully flavored as well as the τ -flavored regimes. We find that

$$\varepsilon_1^e = 0, \quad (3.11)$$

while

$$\varepsilon_1^\mu = \xi [b_2 k^2 (\chi_1 + \chi_2) + b_1 (\chi_3 + \chi_4) - b_1^2 \chi_5] = -\varepsilon_1^\tau. \quad (3.12)$$

In (3.12) the real parameters ξ and χ_i ($i = 1 - 5$) are defined as

$$\begin{aligned} \xi &= \frac{1}{4[b_1^2 + (a^2 + b_1^2 + b_2^2)k^2 + b_2^2 k^4] \pi v^2}, \\ \chi_1 &= b_2(1 + k^2)[c_1 c_2 \{1 + g(x_{12}) - x_{12}\} + d_1 d_2 \{1 + g(x_{13}) - x_{13}\}], \\ \chi_2 &= a[c_1 e \{1 + g(x_{12}) - x_{12}\} + d_1 f \{1 + g(x_{13}) - x_{13}\}], \\ \chi_3 &= b_2(1 + k^2)[c_1^2 \{1 + g(x_{12}) - x_{12}\} - k^2 [c_2^2 \{1 + g(x_{12}) \\ &\quad - x_{12}\} + d_2^2 \{1 + g(x_{13}) - x_{13}\}] + d_1^2 \{1 + g(x_{13}) - x_{13}\}], \\ \chi_4 &= -a k^2 [c_2 e \{1 + g(x_{12}) - x_{12}\} + d_2 f \{1 + g(x_{13}) - x_{13}\}], \\ \chi_5 &= k^2 [c_1 c_2 \{1 + g(x_{12}) - x_{12}\} + d_1 d_2 \{1 + g(x_{13}) - x_{13}\}]. \end{aligned} \quad (3.13)$$

Thus the nonzero leptonic CP asymmetry parameter $\varepsilon_1^\mu = -\varepsilon_1^\tau$ depends on all ten parameters of m_D^{CES} as well as on x_{12} and x_{13} .

We had earlier identified $\text{Im } m_D^{CES}$ as the common source of the origin of a nonzero θ_{13} and leptonic CP violation. A real m_D^{CES} implies vanishing values for b_2 , c_2 and d_2 in which case $\varepsilon_1^\mu = -\varepsilon_1^\tau$ vanishes identically and, as explained in Ref. [14], so does θ_{13} . However, the reverse statement is not true. One could have a vanishing leptonic CP asymmetry simply by setting $b_{1,2}$ to zero in (3.12). But, so long as $\text{Im } m_D^{CES}$ is nonzero, e.g. through nonvanishing values of c_2 and d_2 , θ_{13} need not vanish. Indeed, the leptonic CP asymmetry depends rather sensitively on $b_{1,2}$. We shall elaborate on this later in our numerical discussion.

4 Boltzmann equations and baryon asymmetry in different mass regimes

The Boltzmann equations of concern to us govern the evolution of the number densities of the hierarchical heavy neutrinos N_i and the left chiral lepton doublets \mathcal{L}_α . We follow here the treatment given in Ref. [24]. The equations involve decay transitions between N_i and $\mathcal{L}_\alpha \phi$ as well as $\mathcal{L}_\alpha^C \phi^\dagger$ plus scattering transitions $Qu^C \leftrightarrow N_i \mathcal{L}_\alpha$, $\mathcal{L}_\alpha Q^C \leftrightarrow N_i u^C$, $\mathcal{L}_\alpha u \leftrightarrow N_i Q$, $\mathcal{L}_\alpha \phi \leftrightarrow N_i V_\mu$, $\phi^\dagger V_\mu \leftrightarrow N_i \mathcal{L}_\alpha$, $\mathcal{L}_\alpha V_\mu \leftrightarrow N_i \phi^\dagger$. Here Q represents the left-chiral quark doublet with $Q^T = (u_L, d_L)$ and V_μ can stand for either B or $W_{1,2,3}$. We had already introduced in Sec. 1 the variable $z = M_1/T$ and the parametric function $\eta_a(z)$. When in thermal equilibrium, the latter is denoted by $\eta_a^{\text{eq}}(z)$. Recall that the number density of a particle of species a and mass m_a with g_a internal degrees of freedom is given by [25]

$$n_a(T) = \frac{g_a m_a^2 T}{2\pi^2} \frac{e^{\mu_a(T)/T}}{K_2\left(\frac{m_a}{T}\right)}, \quad (4.1)$$

K_2 being the modified Bessel function of the second kind with order 2. The corresponding equilibrium density, as given by setting the chemical potential $\mu_a(T)$ equal to zero, is

$$n_a^{\text{eq}}(T) = \frac{g_a m_a^2 T}{2\pi^2} K_2\left(\frac{m_a}{T}\right). \quad (4.2)$$

We are now in a position to make use of the Boltzmann evolution equations given in Ref. [24] – generalized with flavor [26]. In making this generalization, one comes across a subtlety: the active flavor in the mass

regime (given by the value of M_1) under consideration may not be individually e , μ or τ but some combination thereof. So we use a general flavor index λ for the lepton asymmetry. Now we write

$$\begin{aligned}\frac{d\eta_{N_i}}{dz} &= \frac{z}{H(z=1)} \left[\left(1 - \frac{\eta_{N_i}}{\eta_{N_i}^{\text{eq}}}\right) \sum_{\beta=e,\mu,\tau} \left(\Gamma^{\beta Di} + \Gamma_{\text{Yukawa}}^{\beta Si} + \Gamma_{\text{Gauge}}^{\beta Si} \right) \right. \\ &\quad \left. - \frac{1}{4} \sum_{\beta=e,\mu,\tau} \eta_L^\beta \varepsilon_i^\beta \left(\Gamma^{\beta Di} + \tilde{\Gamma}_{\text{Yukawa}}^{\beta Si} + \tilde{\Gamma}_{\text{Gauge}}^{\beta Si} \right) \right], \\ \frac{d\eta_L^\lambda}{dz} &= -\frac{z}{H(z=1)} \left[\sum_{i=1}^3 \varepsilon_i^\lambda \left(1 - \frac{\eta_{N_i}}{\eta_{N_i}^{\text{eq}}}\right) \sum_{\beta=e,\mu,\tau} \left(\Gamma^{\beta Di} + \Gamma_{\text{Yukawa}}^{\beta Si} + \Gamma_{\text{Gauge}}^{\beta Si} \right) \right. \\ &\quad \left. + \frac{1}{4} \eta_L^\lambda \left\{ \sum_{i=1}^3 \left(\Gamma^{\lambda Di} + \Gamma_{\text{Yukawa}}^{\lambda Wi} + \Gamma_{\text{Gauge}}^{\lambda Wi} \right) + \Gamma_{\text{Yukawa}}^{\lambda \Delta L=2} \right\} \right].\end{aligned}\quad (4.3)$$

In each RHS of (4.3), apart from the Hubble rate of expansion H at the decay temperature, we have various transition widths Γ originally introduced in Ref. [25] which are linear combinations (normalized to the photon density) of different CP conserving collision terms γ_Y^X for the transitions $X \rightarrow Y$ and $\bar{X} \rightarrow \bar{Y}$. Here γ_Y^X is defined as

$$\gamma_Y^X \equiv \gamma(X \rightarrow Y) + \gamma(\bar{X} \rightarrow \bar{Y}), \quad (4.4)$$

with

$$\gamma(X \rightarrow Y) = \int d\pi_X d\pi_Y (2\pi)^4 \delta^{(4)}(p_X - p_Y) e^{-p_X^0/T} |\mathcal{M}(X \rightarrow Y)|^2. \quad (4.5)$$

In (4.5) one has used a short hand notation for the phase space

$$d\pi_x = \frac{1}{S_x} \prod_{i=1}^{n_x} \frac{d^4 p_i}{(2\pi)^3} \delta(p_i^2 - m_i^2) \theta(p_i^0) \quad (4.6)$$

with $S_X = n_{id}!$ being a symmetry factor in case the initial state X contains a number n_{id} of identical particles. Moreover, the squared matrix element in (4.5) is summed (not averaged) over the internal degrees of freedom of the initial and final states.

The transition widths Γ in (4.3) are given as follows:

$$\Gamma^{\lambda Di} = \frac{1}{n_\gamma} \gamma_{\mathcal{L}_\lambda \phi^\dagger}^{N_i}, \quad (4.7)$$

$$\Gamma_{\text{Yukawa}}^{\lambda Si} = \frac{1}{n_\gamma} \left(\gamma_{Qu^C}^{N_i \mathcal{L}_\lambda} + \gamma_{\mathcal{L}_\lambda Q^C}^{N_i u^C} + \gamma_{\mathcal{L}_\lambda u}^{N_i Q} \right), \quad (4.8)$$

$$\tilde{\Gamma}_{\text{Yukawa}}^{\lambda Si} = \frac{1}{n_\gamma} \left(\frac{\eta_{N_i}}{\eta_{N_i}^{\text{eq}}} \gamma_{Qu^C}^{N_i \mathcal{L}_\lambda} + \gamma_{\mathcal{L}_\lambda Q^C}^{N_i u^C} + \gamma_{\mathcal{L}_\lambda u}^{N_i Q} \right), \quad (4.9)$$

$$\Gamma_{\text{Gauge}}^{\lambda Si} = \frac{1}{n_\gamma} \left(\gamma_{\mathcal{L}_\lambda \phi}^{N_i V_\mu} + \gamma_{\phi^\dagger V_\mu}^{N_i \mathcal{L}_\lambda} + \gamma_{\mathcal{L}_\lambda V_\mu}^{N_i \phi^\dagger} \right), \quad (4.10)$$

$$\tilde{\Gamma}_{\text{Gauge}}^{\lambda Si} = \frac{1}{n_\gamma} \left(\gamma_{\mathcal{L}_\lambda \phi}^{N_i V_\mu} + \frac{\eta_{N_i}}{\eta_{N_i}^{\text{eq}}} \gamma_{\phi^\dagger V_\mu}^{N_i \mathcal{L}_\lambda} + \gamma_{\mathcal{L}_\lambda V_\mu}^{N_i \phi^\dagger} \right), \quad (4.11)$$

$$\Gamma_{\text{Yukawa}}^{\lambda Wi} = \frac{2}{n_\gamma} \left(\gamma_{Qu^C}^{N_i \mathcal{L}_\lambda} + \gamma_{\mathcal{L}_\lambda Q^C}^{N_i u^C} + \gamma_{\mathcal{L}_\lambda u}^{N_i Q} + \frac{\eta_{N_i}}{2\eta_{N_i}^{\text{eq}}} \gamma_{Qu^C}^{N_i \mathcal{L}_\lambda} \right), \quad (4.12)$$

$$\Gamma_{\text{Gauge}}^{\lambda Wi} = \frac{2}{n_\gamma} \left(\gamma_{\mathcal{L}_\lambda \phi}^{N_i V_\mu} + \gamma_{\phi^\dagger V_\mu}^{N_i \mathcal{L}_\lambda} + \gamma_{\mathcal{L}_\lambda V_\mu}^{N_i \phi^\dagger} + \frac{\eta_{N_i}}{2\eta_{N_i}^{\text{eq}}} \gamma_{\phi^\dagger V_\mu}^{N_i \mathcal{L}_\lambda} \right), \quad (4.13)$$

$$\Gamma_{\text{Yukawa}}^{\lambda \Delta L=2} = \frac{2}{n_\gamma} \sum_{\beta=e,\mu,\tau} \left(\gamma_{\mathcal{L}_\beta^C \phi^\dagger}^{N_i \mathcal{L}_\lambda \phi} + 2\gamma_{\phi^\dagger \phi^\dagger}^{N_i \mathcal{L}_\lambda \mathcal{L}_\beta} \right). \quad (4.14)$$

The explicit expressions for γ and γ' are given in Appendix B of Ref. [24]. The subscripts D , S and W stand for decay, scattering and washout respectively. We rewrite the Boltzmann equations in terms of $Y_{N_i}(z) = \eta_{N_i}(z)s^{-1}$ and certain D -functions of z that are defined below.

Consider the first equation in (4.3) to start with. Its second RHS term has been neglected for our assumed hierarchical leptogenesis since both η_L^β and ε_i^β are each quite small and their product much smaller³. Using some shorthand notation, as explained in Eqs. (4.16) - (4.18) below, we can now write

$$\frac{dY_{N_i}(z)}{dz} = \{D_i(z) + D_i^{\text{SY}}(z) + D_i^{\text{SG}}(z)\} \{(Y_{N_i}^{\text{eq}}(z) - Y_{N_i}(z))\}, \quad (4.15)$$

³In order of magnitude this product is $10^{-6} \times 10^{-5} \sim 10^{-11}$, as compared with the first term which is $\mathcal{O}(1)$.

where

$$D_i(z) = \sum_{\beta=e,\mu,\tau} D_i^\beta(z) = \sum_{\beta=e,\mu,\tau} \frac{z}{H(z=1)} \frac{\Gamma^{\beta Di}}{\eta_{N_i}^{\text{eq}}(z)}, \quad (4.16)$$

$$D_i^{\text{SY}}(z) = \sum_{\beta=e,\mu,\tau} \frac{z}{H(z=1)} \frac{\Gamma_{\text{Yukawa}}^{\beta Si}}{\eta_{N_i}^{\text{eq}}(z)}, \quad (4.17)$$

$$D_i^{\text{SG}}(z) = \sum_{\beta=e,\mu,\tau} \frac{z}{H(z=1)} \frac{\Gamma_{\text{Gauge}}^{\beta Si}}{\eta_{N_i}^{\text{eq}}(z)}. \quad (4.18)$$

Turning to the second equation in (4.3) and neglecting the $\Delta L = 2$ scattering terms, we rewrite it as

$$\begin{aligned} \frac{d\eta_L^\lambda(z)}{dz} = & - \sum_{i=1}^3 \varepsilon_i^\lambda \{ D_i(z) + D_i^{\text{SY}}(z) + D_i^{\text{SG}}(z) \} (\eta_{N_i}^{\text{eq}}(z) - \eta_{N_i}(z)) \\ & - \frac{1}{4} \eta_L^\lambda \sum_{i=1}^3 \left\{ \frac{1}{2} D_i^\lambda(z) z^2 K_2(z) + D_i^{\lambda \text{YW}}(z) + D_i^{\lambda \text{GW}}(z) \right\} \end{aligned} \quad (4.19)$$

with

$$D_i^{\text{YW}}(z) = \sum_{\beta=e,\mu,\tau} \frac{z}{H(z=1)} \Gamma_{\text{Yukawa}}^{\beta Wi}, \quad (4.20)$$

$$D_i^{\text{GW}}(z) = \sum_{\beta=e,\mu,\tau} \frac{z}{H(z=1)} \Gamma_{\text{Gauge}}^{\beta Wi}. \quad (4.21)$$

A major simplification (4.19) occurs in our model when the active flavor λ equals e since $\varepsilon_1^e = 0$ and only the second RHS term contributes to the evolution of η^λ . Then the solution of the equation becomes [27]

$$\eta_L^e(z) = \eta_L^e(z=0) \exp\left[-\frac{1}{4} \int_0^z W^e(z') dz'\right], \quad (4.22)$$

where

$$W^e(z) = \frac{1}{2} D_1^e(z) z^2 K_2(z) + D_1^{e \text{YW}}(z) + D_1^{e \text{GW}}(z). \quad (4.23)$$

However, at a very high temperature, the lepton asymmetries get efficiently washed out. Therefore $\eta_L^e(z \rightarrow 0)$ vanishes and from (4.22) $\eta_L^e(z) = 0$ for all z . Similarly, for an unflavored (i.e flavor-summed) leptogenesis in our model, $\eta^e + \eta^\mu + \eta^\tau = 0$ since $\varepsilon_1^\mu = -\varepsilon_1^\tau$.

We are now ready to calculate the baryon asymmetry from the lepton asymmetry. To that end, it is first convenient to define the variable

$$Y_\lambda = \frac{n_L^\lambda - n_{\bar{L}}^\lambda}{s} = \frac{n_\gamma}{s} \eta_L^\lambda, \quad (4.24)$$

i.e. the leptonic minus the antileptonic number density of the active flavor λ normalized to the entropy density. The factor s/η_γ is known to equal $1.8g_{*s}$ and is a function of temperature. For $T > 10^2$ GeV, g_{*s} is known to remain nearly constant with temperature at a value (with three right chiral neutrinos) of about 112 [28]. Sphaleronic processes convert the lepton asymmetry created by the decay of the right chiral heavy neutrinos into a baryon asymmetry by keeping $\Delta_\lambda = \frac{1}{3}B - L^\lambda$ conserved. Y_{Δ_λ} , defined as $s^{-1}\{1/3(n_B - n_{\bar{B}}) - (n_L - n_{\bar{L}})\}$, and Y_λ are linearly related, as under

$$Y_\lambda = \sum_\rho A_{\lambda\rho} Y_{\Delta_\rho}, \quad (4.25)$$

where $A_{\lambda\rho}$ are a set of numbers whose values depend on which of the three mass regimes in which M_1 lies, as mentioned in the Introduction. These are discussed in detail later in the section. Meanwhile, we can rewrite (4.19) as

$$\begin{aligned} \frac{dY_{\Delta_\lambda}}{dz} = & \sum_{i=1}^3 [\varepsilon_i^\lambda \{ D_i(z) + D_i^{\text{SY}}(z) + D_i^{\text{SG}}(z) \} \{ Y_{N_i}^{\text{eq}}(z) - Y_{N_i}(z) \}] \\ & + \frac{1}{4} \sum_\rho A_{\lambda\rho} Y_{\Delta_\rho} \sum_{i=1}^3 \left\{ \frac{1}{2} D_i^\lambda(z) z^2 K_2(z) + D_i^{\lambda \text{YW}}(z) + D_i^{\lambda \text{GW}}(z) \right\}. \end{aligned} \quad (4.26)$$

We need to solve (4.15) and (4.26) and evolve Y_{N_i} as well as Y_{Δ_λ} upto a value of z where the quantities Y_{Δ_λ} become constant with z , i.e. do not change as z is varied. The final baryon asymmetry Y_B is obtained [29] linearly in terms Y_{Δ_λ} , the coefficient depending on the mass regime in which M_1 is located, as explained in what follows. Let us then discuss three mass regimes separately.

4.1 $M_1 < 10^9$ GeV

Here all three lepton flavors are separately distinguishable. Therefore the flavor index λ can just be $\lambda = e$ or μ or τ . In this case the 3×3 A matrix, whose λ, ρ element relates Y_λ and Y_{Δ_ρ} , is given by [7]

$$A = \begin{pmatrix} -151/179 & 20/179 & 20/179 \\ 25/358 & -344/537 & 14/537 \\ 25/358 & 14/537 & -344/537 \end{pmatrix}. \quad (4.27)$$

Now the final baryon asymmetry normalized to the entropy density, is given by [30]

$$Y_B = \frac{28}{79}(Y_{\Delta_\mu} + Y_{\Delta_\tau}), \quad (4.28)$$

since Y_{Δ_e} vanishes on account of η_L^e being zero. Another important parameter, namely the baryon asymmetry normalized to the photon density, obtains as

$$\eta_B = \left. \frac{s}{n_\gamma} \right|_0 Y_B = 7.0394 Y_B, \quad (4.29)$$

the subscript zero denoting the present epoch.

4.2 10^9 GeV $< M_1 < 10^{12}$ GeV

In this regime the τ flavor is distinguishable but one cannot differentiate between the e and μ flavors. It is therefore convenient to define two sets of CP asymmetry parameters ε^τ and $\varepsilon^{(2)} = \varepsilon^e + \varepsilon^\mu$. Therefore the index λ takes the values τ and 2. The Boltzmann equations lead to the two asymmetries Y_{Δ_τ} and Y_{Δ_2} . These are related to Y_τ and $Y_2 = Y_e + Y_\mu$ by a 2×2 A-matrix given by [7]

$$A = \begin{pmatrix} -417/589 & 120/589 \\ 30/589 & -390/589 \end{pmatrix}. \quad (4.30)$$

The final baryon asymmetry Y_B is then calculated as [7]

$$Y_B = \frac{28}{79}(Y_{\Delta_2} + Y_{\Delta_\tau}). \quad (4.31)$$

4.3 $M_1 > 10^{12}$ GeV

In this case all the lepton flavors act indistinguishably leading to a single CP asymmetry parameter $\varepsilon_i = \sum_\lambda \varepsilon_i^\lambda$. As mentioned earlier, $\sum_\lambda \eta_L^\lambda = 0$ and $Y_\Delta = 0$. Therefore $Y_B = 0$ and no baryogenesis is possible in this mass regime. This statement is independent of the mass ordering of the light neutrinos.

5 Numerical analysis: methodology and discussion

In order to numerically check the viability of our theoretical results, the allowed (3σ) values of globally fitted neutrino oscillation data [31] and the upper bound of 0.23 eV on the sum of the light neutrino masses have been used, cf. Table 3. We first constrain the parameter space constructed with the six rescaled parameters defined in Eqs. (2.17) - (2.20). Both normal and inverted types of light neutrino mass ordering are found to be allowed over a sizable region of the parameter space consistent with the input constraints. The ranges of

Table 3: Input values used

Parameters	θ_{12} degrees	θ_{23} degrees	θ_{13} degrees	Δm_{21}^2 10^{-5}eV^2	$ \Delta m_{31}^2 $ $10^{-3}(\text{eV}^2)$	$\sum_i m_i$ (eV)
3σ ranges/ others	31.29 – 35.91	38.3 – 53.3	7.87 – 9.11	7.02 – 8.09	2.32 – 2.59	< 0.23
Best fit values (NO)	33.48	42.3	8.50	7.50	2.46	–
Best fit values (IO)	33.48	49.5	8.51	7.50	2.45	–

the rescaled parameters are graphically shown in Fig.2 and Fig.3 respectively for the normal and the inverted ordering of the light neutrino masses. This is the primary constraining procedure since the CP asymmetry parameters ε_i^α and the different Γ 's of the Boltzmann equations depend individually upon the elements of m_D and the RH neutrino masses M_i ($i = 1, 2, 3$). Therefore, merely restricting the rescaled parameters is not sufficient for the computation of the final baryon asymmetry. In order to obtain the allowed ranges of

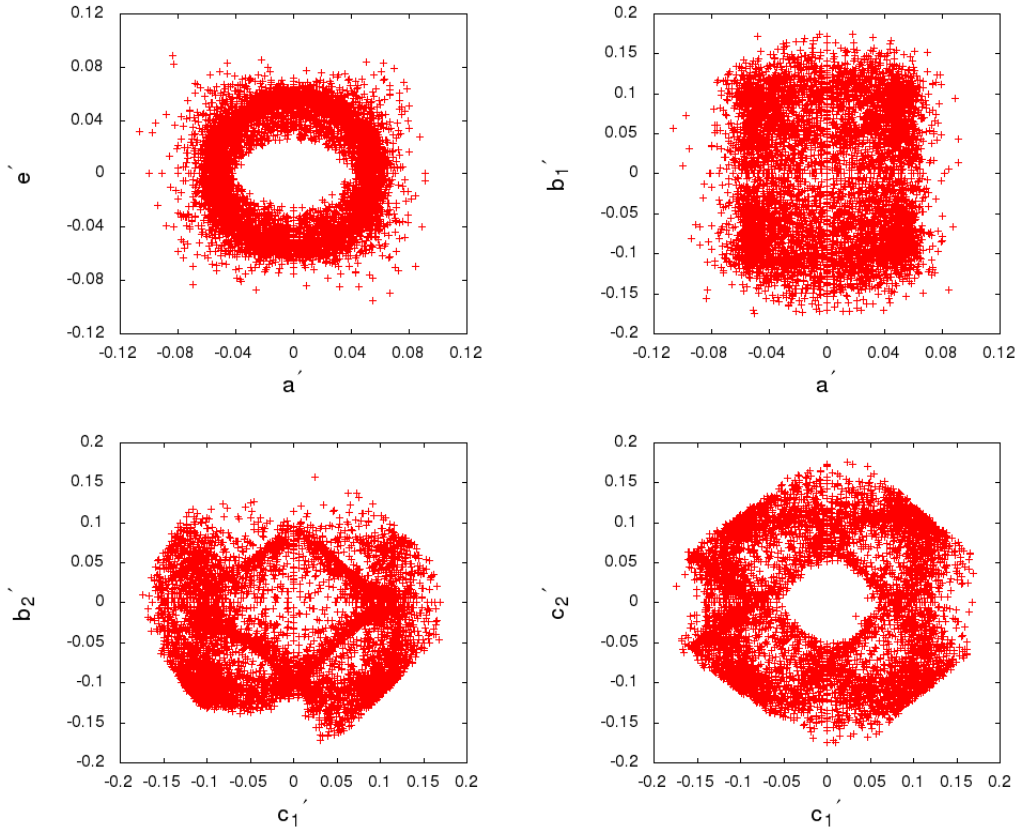


Figure 2: Plots of the reduced parameters for a normal mass ordering of the light neutrinos.

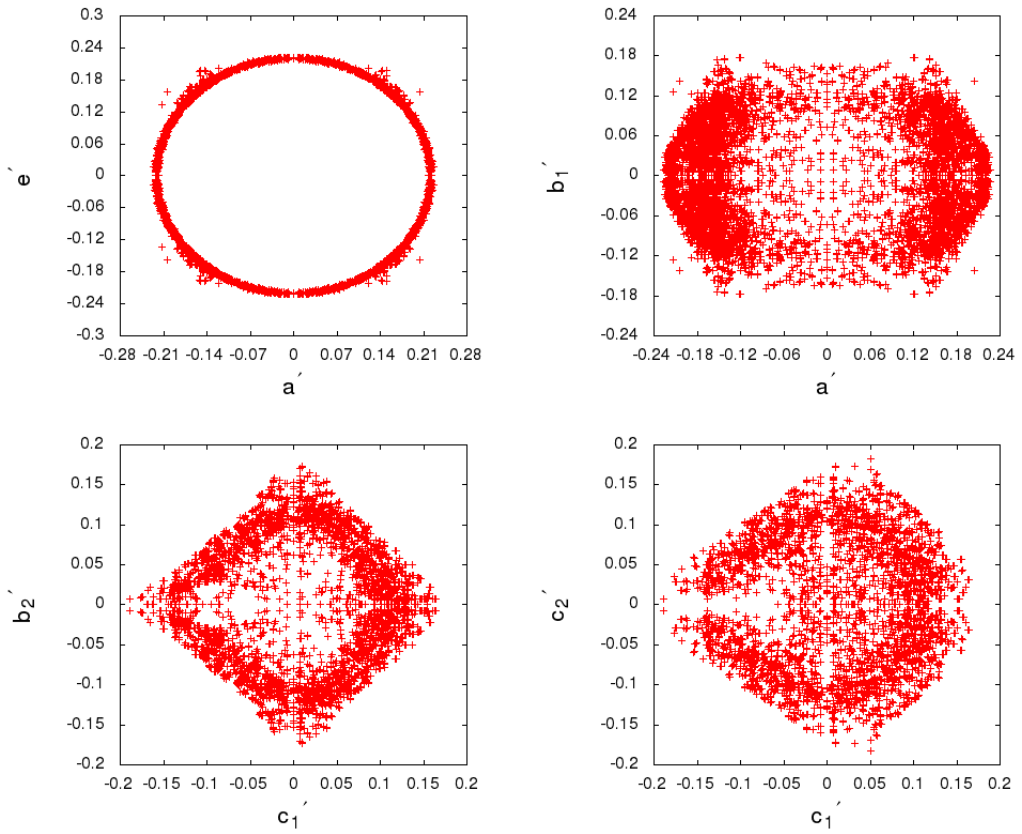


Figure 3: Plots of the reduced parameters for an inverted mass ordering of the light neutrinos.

the parameters a , $b_{1,2}$, $c_{1,2}$ and e , included in m_D , we incorporate the strong hierarchy assumption of the RH neutrino masses ($M_1 \ll M_2 \ll M_3$), as mentioned in earlier sections. For numerical purposes, we arbitrarily choose $M_2/M_1 = M_3/M_2 = 10^3$. We shall later discuss in Section 6 the effects of changing these mass ratios. Depending upon the mass regime, for a fixed value of M_1 , we then obtain the allowed ranges of the parameters of m_D from the relations defined in Eqs. (2.17) - (2.20).

Even after constraining the six unprimed parameters of m_D and the masses of the three right handed heavy neutrinos, three undetermined parameters remain – namely f , d_1 and d_2 . The latter have been neglected earlier in the primary implementation of the input constraints since their contributions to the light neutrino mass matrix M_ν are suppressed by the heaviest RH neutrino mass M_3 . However, for a quantitatively successful treatment of leptogenesis, one needs to estimate these missing parameters too, as mentioned in Sec. 2. We discuss here some technical details regarding this estimation. For example, let us consider the first equation of Table 1, namely

$$x = -\left(\frac{a^2}{M_1} + \frac{e^2}{M_2} + \frac{f^2}{M_3}\right). \quad (5.1)$$

The last RHS term was earlier neglected on the grounds that the parameter f , which is presumably of same the order of magnitude as a or e , is suppressed by M_3 . Now, in order to estimate f , we first set it at a value which is larger i.e. between a and e . Then we keep on decreasing it until the quantity $f^2 M_3^{-1}/(a^2 M_1^{-1} + e^2 M_2^{-1})$ becomes less than a very small number which we choose to be 10^{-5} . In a similar manner one can estimate approximate values of d_1 and d_2 . Thus, knowing the numerical values of all the parameters of m_D as well as those of M_R , we can make a realistic estimate of the final value of the baryon asymmetry. The first step towards the last-mentioned goal is the estimation of ε_1^λ in the three mass regimes of M_1 . We have carried out our numerical analysis over a wide range of values of M_1 in the τ -flavored and in the fully flavored regimes. As mentioned in the last paragraph of Sec. 3, $\varepsilon_1^{\mu,\tau}$ are mostly sensitive to $b_{1,2}$. In order to see the nature of the variation of $\varepsilon_1^{\mu,\tau}$ with $b_{1,2}$ for constant values of c_2 and d_2 , we first set c_2 and d_2 to be zero. Now the simplified expression of the relevant CP asymmetry parameter becomes

$$\varepsilon_1^\mu = \xi(b_2 k^2 \chi_2 + b_1 \chi_3') = -\varepsilon_1^\tau, \quad (5.2)$$

where ξ and χ_2 as are defined in (3.13), and χ_3' is given by

$$\chi_3' = b_2(1 + k^2)[c_1^2\{1 + g(x_{12}) - x_{12}\} + d_1^2\{1 + g(x_{13}) - x_{13}\}]. \quad (5.3)$$

For a graphical representation of the variation of the CP asymmetry parameter ε_1^μ with $b_{1,2}$, we choose a sample value of $M_1 = 3.62 \times 10^{11}$ GeV and assume a normal mass ordering⁴ of the light neutrinos. The corresponding scatter plots are shown in Fig. 4. The vanishing of $b_{1,2}$ implies $\varepsilon_1^\mu = 0$; therefore, in our

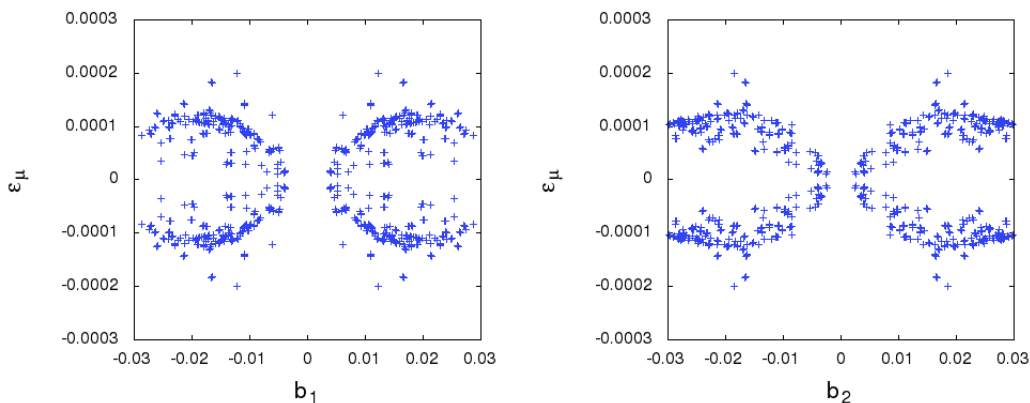


Figure 4: Plot of ε_1^μ with b_1 (left), b_2 (right) for a normal light neutrino mass ordering.

numerical computation, only those values of ε_1^μ are allowed which correspond to $b_{1,2} \neq 0$. One can have a similar plot for ε_1^τ since $\varepsilon_1^\mu = -\varepsilon_1^\tau$ and the plots in Fig. 4 are symmetric about the origin. The corresponding plots for an inverted mass ordering of the light neutrinos can also be generated. However, with the same computational technique as used for normal ordering, we find a much smaller number of allowed points which hardly show a fair variation of ε_1^μ with $b_{1,2}$.

⁴ As we shall see later, in our model an inverted mass ordering is disfavored in terms of a realistic baryogenesis.

Finally, knowing the numerical range of ε_1^λ is the last step needed to solve the Boltzmann equations given in (4.15) and (4.26) leading to the parameter Y_{Δ_λ} upto a fairly large value of z where Y_{Δ_λ} becomes constant. Then, using the suitable equations (4.28), (4.31), depending upon the energy regime, one can compute the final value of Y_B . However, this final step needs to overcome the following hurdle. Unlike estimating ε_1^λ for the entire allowed parameter ranges of m_D and M_R , it becomes impractical in terms of computer time to solve the Boltzmann equations for this huge data set even if M_1 is fixed to a constant value. So we were obliged to use only those values of the members of parameter set for which the neutrino oscillation observables are restricted close to their best fit values. For this purpose we choose a χ^2 for every observable deviating from its experimentally measured best fit value as

$$\chi^2 = \sum_{i=1}^5 \left[\frac{O_i(th) - O_i(bf)}{\Delta O_i} \right]. \quad (5.4)$$

In (5.4) O_i denotes the i th neutrino oscillation observable from among $(\Delta m_{21}^2, \Delta m_{32}^2, \theta_{12}, \theta_{23}, \theta_{13})$ and the summation runs over all the five observables. The parenthetical *th* stands for the theoretical prediction, i.e the numerical value of the observable given by our model, whereas *bf* denotes the best fit value (cf. Table 3). ΔO_i in the denominator stands for the measured 1σ range of O_i . After calculating χ^2 for all the points $\{a', e', b'_1, c'_1, b'_2, c'_2\}$, as allowed by the oscillation data, we start from the minimum value of the χ^2 ($= \chi_{min}^2$) and keep on increasing the latter until we get Y_B to be positive as well as in the observed range. It is to be noted that for a particular value of χ^2 , i.e. for a particular primed data set, we are able to generate a large number of unprimed points (parameters of m_D) by varying the values of M_1 in Eqs. (2.17)-(2.20). To be more precise, ' n ' values of M_1 lead to ' n ' values of the unprimed set of parameters for the particular primed set under consideration. The other three parameters f , d_1 and d_2 are again computed by means of the previously mentioned approximation technique. We vary M_1 over a wide range in the relevant mass regimes for both types of mass ordering and present our final result systematically in the following way.

Y_B for normal mass ordering of light neutrinos:

$M_1 < 10^9$ GeV: In this regime all lepton flavors (e, μ, τ) act distinguishably. However, since $\varepsilon_1^e = 0$, we first need to evaluate $\varepsilon_1^{\mu, \tau}$ individually. It is found that $|\varepsilon_1^{\mu, \tau}|$ can have values at most $\sim 10^{-8}$. Y_B of the right amount cannot be generated with such a small CP asymmetry parameter [5].

10^9 GeV $< M_1 < 10^{12}$ GeV: After carrying out the χ^2 analysis for this regime, we first calculate the final Y_B for $\chi_{min}^2 (= 0.002)$. It is found that the final Y_B saturates to a negative value. Then we keep on increasing χ^2 and find that a positive value for the final Y_B within the observed range may be obtained for $\chi^2 = 0.003$ which is close enough to the best-fit value of $\chi^2 = 0.002$. In the entire analysis, for each value of χ^2 , i.e. for this single primed set, M_1 is varied over a wide range. Then, for each value of M_1 , a set of values of the unprimed parameters $\{a, e, f, b_1, c_1, d_1, b_2, c_2, d_2\}$ is generated. The Boltzmann equations are solved for each set of values of M_1 . Since, in this regime, the τ flavor acts distinguishably, we need to solve

Table 4: parameters corresponding $\chi^2 = 0.003$ for normal mass ordering.

a'	e'	b'_1	c'_1	b'_2	c'_2	χ^2
0.026	0.054	0.019	0.095	-0.080	0.095	0.003

the Boltzmann equations for two flavors (τ and 2) in order to obtain the variation of $Y_{\Delta_{\tau,2}}$ or of Y_B with z . For each set of the primed parameters, we take thirty values of M_1 within the range 10^9 GeV to 10^{12} GeV and solve the Boltzmann equations thirty times for each M_1 along with the corresponding unprimed set of rescaled parameters. For a concise presentation, in Table 5, we tabulate only ten such values of M_1 for which Y_B is near or inside the observed range. Fig.5 contains a graphical presentation of the variation of

Table 5: Y_B for different masses of lightest right handed neutrino.

$\frac{M_1}{10^{11}}$ (GeV)	3.57	3.58	3.59	3.60	3.61	3.62	3.63	3.64	3.65	3.66
$Y_B \times 10^{11}$	8.55	8.57	8.59	8.61	8.64	8.66	8.69	8.71	8.74	8.77

the asymmetries Y_{Δ_2} , Y_{Δ_τ} and Y_B with z for a definite value of M_1 which is taken to be 3.62×10^{11} GeV. It may be seen that Y_B is inside the observed range [1] for large z corresponding to the present epoch. A

careful surveillance of Table 5 leads to the conclusion that we can obtain upper and lower bounds on M_1 due to the constraint from the observed range of Y_B . One can appreciate this fact more clearly from the plot of Y_B vs. M_1 in Fig.6. Two straight lines have been drawn parallel to the abscissa in Fig.6: one at $Y_B = 8.55 \times 10^{-11}$ and the other at $Y_B = 8.77 \times 10^{-11}$. The values of M_1 , where the straight lines meet the Y_B vs z curve, yield the allowed lower and upper bounds on M_1 , namely $(M_1)_{lower} = 3.57 \times 10^{11}$ GeV and $(M_1)_{upper} = 3.66 \times 10^{11}$ GeV.

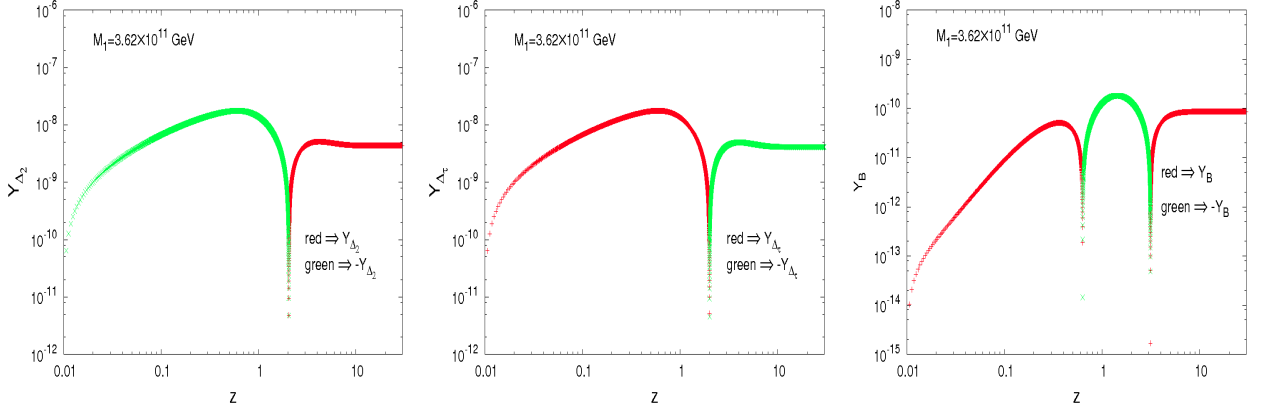


Figure 5: Variation of Y_{Δ_μ} (left), Y_{Δ_τ} (middle), Y_B (right) with z in the mass regime (2) for a definite value of M_1 . N.B. since these become negative for certain values of z , their negatives have been plotted on the log scale for those values of z . A normal mass ordering for the light neutrinos has been assumed.

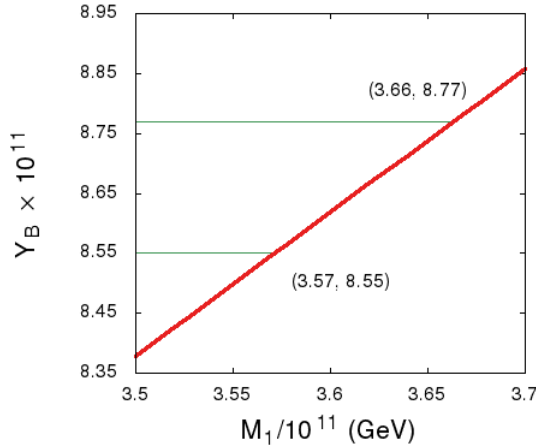


Figure 6: A plot of the final Y_B for different values of M_1 for a normal light neutrino mass ordering.

$M_1 > 10^{12}$ GeV: It has been shown that $Y_B = 0$ here for our model.

Y_B for inverted mass ordering of light neutrinos:

In this case too the numerical estimation of the baryon asymmetry parameter has been made exactly in the same manner as for a normal mass ordering. A final discussion for each regime goes as follows.

$M_1 < 10^9$ GeV: As in the case of normal ordering, the values of $\varepsilon_1^{\mu,\tau}$ can reach up to at most the order of 10^{-8} which is not adequate to let Y_B come within its observed range.

10^9 GeV $< M_1 < 10^{12}$ GeV: In this regime we first calculate the minimum value of χ^2 for the full set of primed parameters constrained by the oscillation data. We find that for $\chi_{min}^2 = 0.246$ the final baryon asymmetry saturates to a negative value. As in the previous case we then keep on increasing the value of χ^2 and check the final Y_B by varying M_1 over a wide range for each value of χ^2 . It turns out that though Y_B attains a positive value for $\chi^2 = 0.952$, it is below the observed range. Then, using the χ^2 enhancement

technique, for Y_B to be in the observed range the minimum value of χ^2 is found to be 1.67 which is far away from the best-fit point. The set of primed parameters for $\chi^2 = 1.67$ is tabulated in Table 6.

Table 6: parameters corresponding $\chi^2 = 1.67$ for inverted hierarchy

a'	e'	b'_1	c'_1	b'_2	c'_2	χ^2
0.15	0.16	-0.017	-0.022	0.10	-0.096	1.67

$M_1 > 10^{12}$ GeV: Once again, $Y_B = 0$ here for the present model.

A compact presentation of the final conclusions regarding Y_B from the numerical analysis is given in Table 7.

Table 7: Final statements on Y_B for different mass regimes.

Type	$M_1 < 10^9$ GeV	10^9 GeV $< M_1 < 10^{12}$ GeV	$M_1 > 10^{12}$ GeV
Normal Ordering	Ruled out since Y_B is below the observed range for any χ^2 .	Y_B within the observed range for $\chi^2=0.003$ close to $\chi^2_{min} = 0.002$.	Ruled out since $Y_B = 0$.
Inverted Ordering	Ruled out since Y_B is below the observed range for any χ^2 .	Y_B within the observed range for $\chi^2=1.67$ far away from $\chi^2_{min} = 0.246$.	Ruled out since $Y_B = 0$.

We would like to make a further statement before finishing this numerical discussion. Though we had earlier enumerated the difficulties in numerically solving the Boltzmann equations for each data point within the entire 3σ parameter range of m_D , we have been able to perform the task only for a few data points in that range. We actually find that there is no monotonic variation of Y_B with the chosen data points. For example, given a normal ordering of the light neutrino masses, suppose we take the data set that corresponds to the worst fit point (χ^2_{max}) and solve the Boltzmann equations for 10^9 GeV $< M_1 < 10^{12}$ GeV. Such a procedure yields a negative final value of Y_B contrary to the result obtained in the $\chi^2 = 0.003$ case. For the other data points also, Y_B varies widely with the parameters of m_D from one neutrino mass model to another [32–35]. This conclusion is true for all mass regimes (except for $M_1 > 10^{12}$ GeV, where $\sum_{\lambda} \varepsilon_1^{\lambda} = 0$ and hence Y_B vanishes) as well as for an inverted mass ordering of the light neutrinos. Table 7 shows that, for data points close to the best fit values, an inverted mass ordering is not favored in this model. However, *we cannot completely rule out this mass ordering here since such is not the case as one moves further away from the best-fit values while still remaining within the 3σ range.* There may exist certain data sets (e.g. $\chi^2 = 1.67$) in the allowed 3σ ranges for which the proper value of Y_B can be generated even with an inverted light neutrino mass ordering.

6 Sensitivity to the heavier neutrinos

In our analysis so far, the effect of the two heavier neutrinos (N_2, N_3) on the produced final lepton asymmetry has been neglected. We have assumed that the asymmetries produced by the decays of both of them get washed out [36]. We examine this issue in this section. Is Y_B sensitive to N_2 and N_3 ? There are two ways that such a sensitivity might arise: (1) directly, if the contributions to Y_{λ} from $N_{2,3}$ decays do not get washed out for some reason and (2) indirectly, even if those do get washed out, a dependence of Y_B on the heavier RH neutrino masses might persist through the CP asymmetry parameter ε_1^{α} .

Indirect effect of $N_{2,3}$:

Though the neutrino oscillation data have been fitted with the primed parameters, cf (2.17)–(2.20), for computing the quantities related to leptogenesis, we need to examine the unprimed ones, i.e. the Dirac mass matrix elements. Is the final baryon asymmetry affected by the chosen hierarchies of the RH neutrinos? Interestingly, we find that the final Y_B is not so sensitive to $M_{2,3}$. One can justify this statement by simplifying the CP asymmetry parameters of (3.4) to

$$\varepsilon_1^{\alpha} = -\frac{3}{8\pi v^2 \mathcal{H}_{11}} \sum_{j=2,3} \frac{M_1}{M_j} \text{Im}[\mathcal{H}_{1j}(m_D)_{1\alpha}(m_D^*)_{j\alpha}] - \frac{1}{4\pi v^2 \mathcal{H}_{11}} \sum_{j=2,3} \frac{M_1^2}{M_j^2} \text{Im}[\mathcal{H}_{j1}(m_D)_{1\alpha}(m_D^*)_{j\alpha}], \quad (6.1)$$

after approximating $g(x_{1j})$ of Eqs. (3.5) and (3.6) to be $g(x_{1j}) = -\frac{3}{2\sqrt{x_{1j}}}$ for $x_{1j} \gg 1$. The last term of Eq. (6.1) is much suppressed since it is of second order in x_{1j}^{-1} . The first term has two parts for $j = 2, 3$. However, since M_3 is much larger than M_1 and f, d_1 and d_2 are taken to have values of the order of the other Dirac components, the $j = 3$ term has a negligible effect on ε_1^α . Now, for $j = 2$, ε_1^α is simplified as

$$\varepsilon_1^\mu = -\frac{3M_1}{8\pi v^2 \mathcal{H}_{11}} [(ae' + b_1c'_1 + b_2c'_2)(b_2c'_1 + b_1c'_2)] = -\varepsilon_1^\tau \quad (6.2)$$

with $\varepsilon_1^e = 0$. Since e' and $c'_{1,2}$ are fixed by the oscillation data, $\varepsilon_1^{\mu,\tau}$ are insensitive to the value of M_2 . In order to numerically compute the final baryon asymmetry for a normal mass ordering of the light neutrinos, we consider each term in (6.2) and two different mass hierarchical schemes for the RH neutrinos, e.g, $M_{i+1}/M_i = 10^2$ and $M_{i+1}/M_i = 10^4$ where i can take the values 1,2. Recall that in the previous section we have presented Y_B for $M_{i+1}/M_i = 10^3$. A careful inspection of Fig.6 and Fig.7 reveals an interesting fact. Though the chosen mass ratios of the RH neutrinos have been altered, changes in the lower and upper bounds on M_1 are not significant for the observed range of Y_B . For convenience, we present in Table 8 the variation of Y_B with M_1 for different mass ratios.

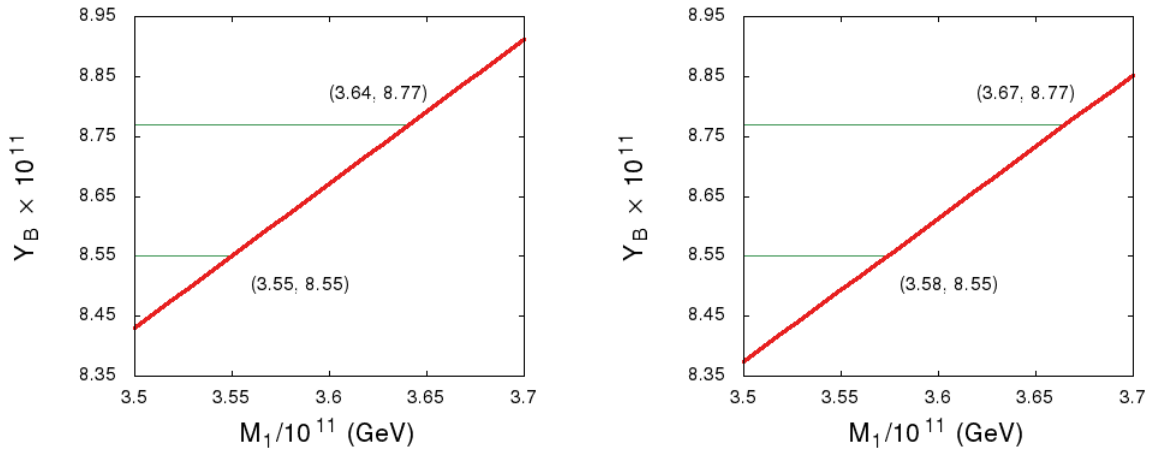


Figure 7: Plots of final Y_B for different values of M_1 for $M_{i+1}/M_i = 10^2$ (left) and $M_{i+1}/M_i = 10^4$ (right).

Table 8: Lower and upper bounds on M_1 for different mass ratios of the RH neutrinos ($i = 1, 2$).

Hierarchies \rightarrow	$M_{i+1}/M_i = 10^2$	$M_{i+1}/M_i = 10^3$	$M_{i+1}/M_i = 10^4$
Upper bound (GeV)	3.64×10^{11}	3.66×10^{11}	3.67×10^{11}
Lower bound (GeV)	3.55×10^{11}	3.57×10^{11}	3.58×10^{11}

Direct effect of N_2 :

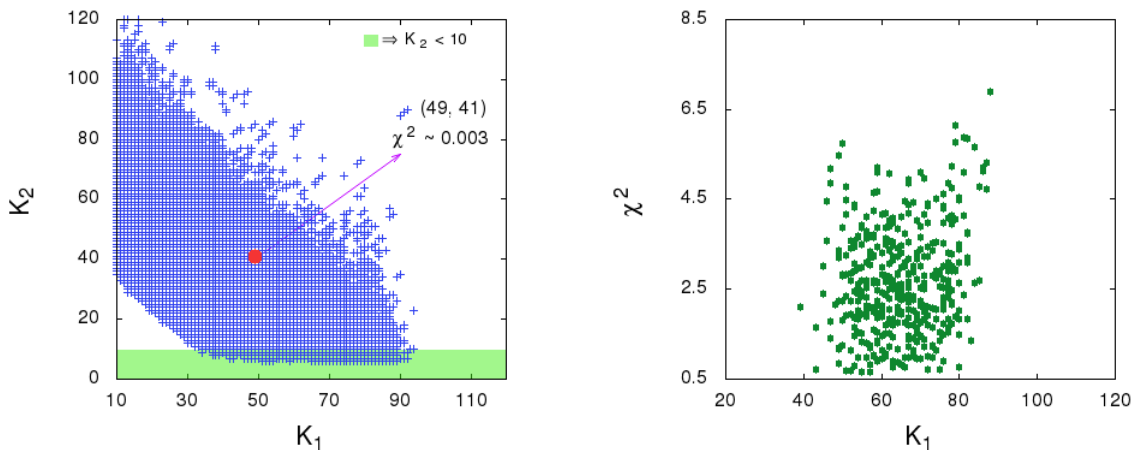


Figure 8: A plot of the two washout parameters K_1 and K_2 appears in the left panel. The red dot corresponds to $\chi^2 = 0.003$ for which we estimate Y_B . The green shaded area indicates a possibility of N_2 leptogenesis. A plot of χ^2 with K_1 for $K_2 < 10$ is given in the right panel. A normal mass ordering for the light neutrinos has been assumed.

Here we consider only N_2 , neglecting N_3 for simplicity. It is argued in Ref. [37] that, due to a decoherence effect [5, 37], a finite lepton asymmetry generated by N_2 decays might remain protected against N_1 -washout and could survive down to the electroweak scale. Thus it itself might generate the final baryon asymmetry if a sizable amount of lepton asymmetry survives. This procedure is subject to the condition that two washout factors K_1 (related to N_1 -washout) and K_2 (related to N_2 -washout) need not be of the same order. These are defined as

$$K_1 = \frac{\mathcal{H}_{11}}{M_1 m^*}, \quad (6.3)$$

$$K_2 = \frac{\mathcal{H}_{22}}{M_2 m^*}, \quad (6.4)$$

where $m^* = 1.66\sqrt{g^*}\pi v^2/M_{Pl} \approx 10^{-3}$ eV. The conditions that are needed can be stated as [37]

$$K_1 \gg 1 \text{ and } K_2 \not\gg 1. \quad (6.5)$$

Here $K_1 \gg 1$ indicates that faster N_1 interactions break coherence among the states produced by N_2 , i.e. a part of the lepton asymmetry produced by N_2 gets protected against N_1 -washout. On the other hand, $K_2 \not\gg 1$ implies a mild washout of the lepton asymmetry produced by N_2 from N_2 -related interactions in a way that a sizable N_2 -generated lepton asymmetry survives during the N_1 -leptogenesis phase. Quantitatively, our allowed parametric region (blue shaded area in the K_2 vs. K_1 plot in the left panel of Fig.8) prefers large values of K_2 in excess of 10 except at the bottom (green band). Thus the $K_2 \not\gg 1$ condition is strongly violated in most of the region. On the other hand, the few allowed points with $K_2 < 10$, displayed in a χ^2 vs. K_1 plot in the right panel of Fig.8, correspond to values of χ^2 above 0.5 far in excess of $\chi^2 = 0.003$ for which we obtain Y_B in the observed range. Therefore, for our calculation, any direct effect of N_2 does not appear to be relevant.

7 Summary and discussion

Some of us has recently proposed [14] a complex-extended scaling model of the light neutrino Majorana mass matrix M_ν , generated by a type-1 seesaw induced by heavy RH neutrinos. Unlike the Simple Real Scaling model advanced earlier [19, 20], this new model can accommodate a nonzero θ_{13} and has a sizable region of parameter space allowed by all current and relevant experimental data [31]. The atmospheric mixing angle θ_{23} is given by $\tan^{-1}(1/k)$, k being a real positive scaling factor which can be either greater or less than unity. Most interesting are the predictions of the model in regard to CP violation: maximal ($\cos \delta = 0$) for the Dirac type and absent ($\alpha, \beta = 0$ or π) for the Majorana type. Since CP violation is crucially related to baryogenesis, we have been motivated in this paper to investigate the latter quantitatively in the model under consideration.

We first performed a general calculation of the CP asymmetries ε_i^α in the decays $N_i \rightarrow \mathcal{L}_\alpha \phi, \mathcal{L}_\alpha^C \phi^\dagger$ in terms of the parameters of the model. This led to a vanishing value of ε_i^e with a generally nonvanishing $\varepsilon_i^\mu = -\varepsilon_i^\tau$. A common source of the origin of a nonzero θ_{13} and these CP asymmetries was found in the imaginary part of m_D . We then evolved $Y_2 = Y_e + Y_\mu$ and Y_τ , respectively equal to $(n_L^{(2)} - n_L^{(2)})/s$ and $(n_L^\tau - n_L^\tau)/s$, from a high temperature (depending on the mass regime in which M_1 lies) down to that of the electroweak phase transition. In doing so we have had to consider the Boltzmann equations for Y_{N_i} and Y_λ , respectively equal to n_{N_i}/s and $(n_L^\lambda - n_L^\lambda)/s$, λ being an active lepton flavor index which can sometimes be a combination of e, μ, τ . We then utilized the different linear relations between Y_λ and Y_{Δ_λ} , with $\Delta_\lambda = \frac{1}{3}B - L_\lambda$, for the three different specified regimes of M_1 to arrive at the baryon asymmetry of the universe for each regime. The latter values have been evaluated numerically and their implications discussed.

In a nutshell, realistic baryogenesis has been found to be possible in this model for values close to best fit values of the input neutrino oscillation observables only in the $10^9 \text{ GeV} < M_1 < 10^{12} \text{ GeV}$ regime and for a normal mass ordering of the light neutrinos. This analysis excludes (from a baryogenesis standpoint) the regimes $M_1 < 10^9 \text{ GeV}$ and $M_1 > 10^{12} \text{ GeV}$ and disfavors an inverted mass ordering of the light neutrinos. However, the latter is still allowed for values of the input parameters away from their best-fit numbers but within a 3σ range. As neutrino oscillation data improve, the conclusions from our analysis will be sharpened.

Acknowledgement

The work of RS and AG is supported by the Department of Atomic Energy (DAE), Government of India. MC acknowledges support from Saha Institute of Nuclear Physics where a part of this work was done. The work of PR has been supported by the Indian National Science Academy.

References

- [1] P.A.R Ade et al. [Planck Collaboration], *Astron. Astrophys.* **594** (2016), A13.
- [2] J.M Cline, arXiv: 0609145 [hep-ph].
- [3] M. Fukugita and T. Yanagida, *Phys. Lett.* **B174** (1986) 45.
- [4] A. Riotto and M. Trodden, *Ann. Rev. Nucl. Part. Sci.* **49** (1999) 35.
- [5] S. Davidson, E Nardi and Y. Nir, *Phys. Rept.* **466** (2008) 105.
- [6] E. Bertuzzo, P.D Bari, F Feruglio and E. Nardi, *JHEP* **0911** (2009) 036.
- [7] A. Abada, S. Davidson, A. Ibarra, F.-X Josse-Michaux, M. Losada and A. Riotto, *JHEP* **0609** (2006) 010.
- [8] S. Antusch, S.F King and A. Riotto, *JCAP* **0611** (2006) 011.
- [9] P. Minkowski, *Phys. Lett.* **67b** (1977) 421.
- [10] M. Gell-Mann, P.Ramond and R. Slansky, *Conf. Proc.* **C790927** (1979) 315.
- [11] T. Yanagida, *Prog. Theor. Phys.* **64** (1980) 1103.
- [12] R.N. Mohapatra, *Phys. Rev. Lett.* **56** (1986) 561.
- [13] A.D Sakharov, *JETP Lett.* **5** (1967) 24.
- [14] R. Samanta, P. Roy and A. Ghosal, *Eur. Phys. J. C* **76** (2016), 662.
- [15] R. Samanta, P. Roy and A. Ghosal, *Acta Phys. Polon. Supp.* **9**, 807 (2016).
- [16] P. Chen, G. J. Ding and S. F. King, *JHEP* **1603**, 206 (2016).
- [17] K.A Olive et al [Particle Data Group] *Chinese Physics C*38, 090001 (2014).
- [18] C.S Lam, *Phys. Lett B* **656**, 193 (2007); *Phys. Rev. Lett.* **101**, 121602 (2008); *Phys. Rev. D* **78**, 073015 (2008).
- [19] L. Lavoura, *Phys. Rev. D* **62**, 093011 (2000).
- [20] R.N Mohapatra and W. Rodejohann, *Phys. Lett. B* **644**, 59 (2007).
- [21] B. Adhikary, M. Chakraborty and A. Ghosal, *Phys. Rev. D* **86**, 013015 (2012).
- [22] A. Ghosal and R. Samanta, *JHEP* **1505**, 077 (2015).
- [23] A.S Joshipura and W. Rodejohann, *Phys. Lett. B* **678**, 276(2009).
- [24] A. Pilaftsis and T.E.J. Underwood, *Nucl. Phys.* **B692** (2004) 392.
- [25] J. Edsjo and P. Gondolo, *Phys. Rev.* **D56** (1997) 1879.
- [26] B. Adhikary, M. Chakraborty and A. Ghosal, *Phys. Rev. D* **93**, 113001 (2016)
- [27] W. Buchmuller, P. Di Bari and M. Plumacher, *Annals Phys.* **315**, 305 (2005).
- [28] E. W Kolb and M.S Turner, *Front. Phys.* **69** (1990)1.
- [29] B. Adhikary, *Phys. Rev.* **D74** (2006) 033002.
- [30] J.A. Harvey and M.S. Turner, *Phys. Rev.* **D42** (1990)3344.
- [31] M. C. Gonzalez-Garcia, M. Maltoni and T. Schwetz, *Nucl. Phys. B* **908**, 199 (2016)
- [32] C. Hagedorn, E. Molinaro and S. T. Petcov, *JHEP* **0909**, 115 (2009).
- [33] S. Blanchet, D. Marfatia and A. Mustafayev, *JHEP* **1011**, 038 (2010).
- [34] M. Borah, D. Borah and M. K. Das, *Phys. Rev. D* **91**, 113008 (2015).
- [35] J. Gehrlein, S. T. Petcov, M. Spinrath and X. Zhang, *Nucl. Phys. B* **899**, 617 (2015).
- [36] W. Buchmuller, P. Di Bari and M. Plumacher, *Nucl. Phys. B* **665**, 445 (2003).
- [37] G. Engelhard, Y. Grossman, E. Nardi and Y. Nir, *Phys. Rev. Lett.* **99**, 081802 (2007).